Proceedings of the
Annual Stability Conference
Structural Stability Research Council
Louisville, Kentucky, April 1-4, 2025

Ultimate flexural capacity of Cold Formed Section Purlins laterally supported by tie rods

M. El Sadawy[1], M. T. Hanna[2], M. Nashaat[3]

Abstract

Cold-formed steel is a competitive solution for many structural applications. Zed "Z" and lipped channel "C" sections are widely used in industrial structures specially as purlins. Purlins are usually placed on inclined plans which cause the vertical loads like dead as well as live loads induce bending moments about the minor axis. Therefore, to reduce the effect of these moments, lateral supports are provided. In this paper, configuration of lateral tie roads connected between parallel purlins that are frequently used in Egypt as lateral support for long span purlins has been studied. First, large scale specimens have been tested experimentally. The tested sections have web depth, flange width, lip depth are 200mm, 60mm, 20mm; respectively. In the tests, purlins are loaded vertically, and the load deformations relations have been recorded until failure. Second, the specimens are simulated numerically using nonlinear finite element model using ABAQUS software. The purlins are modeled as shell elements, while tie rods are modeled as link members. The developed finite element model is validated by comparing its results with the experimental ones. After that, the model is used to make an extended parametric study which includes web width thickness ratios, web-depth to flange width ratios, and number of lateral tie rods. Results reflect that presence of lateral tie rods changing the failure shape of the purlins and enhance its flexural capacity. Finally, the ultimate flexural capacities are compared with that predicted by AISI specifications.

1. Introduction

Cold-formed sections are widely used in structural applications, such as purlins, girts, mainframe members, and roof trusses, because of their high strength-to-weight ratios and ability to be formed into any shape that meets the needs of a given application, Ye, J., Hajirasouliha, et. al.(2016), Guimarães, V. M. et.al. (2021). Cold formed sections are weak in torsional stiffness, and their large width-thickness ratios cause them to fail in three different modes: local, distortional, and global buckling, Zhang, L. and Tong, G. S.(2016). In flexural members, the global buckling is mainly the lateral torsional buckling. In engineering practice, tie rods are commonly employed in purlins to reduce the lateral intervals in order to prevent lateral torsional buckling. The buckling of a single purlin or girt was the primary focus of earlier Studies (Sokol, L.(1996), Basaglia, C., et. al. (2013), Ye, Z.-M., et al. (2002), Chu, X.-T., et al. (2004), Li, L. Y. (2004)). Sun, K., G.Tong,

[1] Professor, Housing and Building National Research Center, <m_massoud2002@yahoo.com>
[2] Professor, Housing and Building National Research Center, <maged.tawfick@hbrc.edu.eg>
[3] Graduate Student, Faculty of Engineering, Shoubra University, <Maro.nashaat@hotmail.com>

and L. Zhang. (2016) studied the impact of the zigzag arrangement of sag rods in nearby bays. They showed that sag-rods bracing effectiveness diminishes with increased spacing from the anchor. They proposed simplified equations for practical design. Tong, G., and Y. Tang. (2017) examined the buckling behavior of a parallel purlin system inter-braced by a single line of tie rods and a single purlin system braced by a tie rod at mid-span, they found that the effective stiffness of the tie rod was a key factor in the relationship between the two systems. Further, the section capacity of Z-purlins with tension flanges restrained by standing seam panels, with and without tie rods, and subject to uplift loading was determined experimentally and numerically by Luan, W., and Li, Y. Q. (2019). Their parameters were two different locations of tie rods and two types of profile sheeting. The results showed that the flexural strength of the purlin system attached with middle tie rods is very close to the Chinese Code. Zhang et. al. (2018) and Zhu et.al. (1999) reported that tie rods could affect the capacity and change the failure modes of channel purlins roof system under uplift uniform load. In addition, lateral braces and corrugated sheeting reduce the lateral as well as torsional deformations and increase the ultimate loading capacity. Zhang, Y. C., & Wang, H. M. (2009) suggested the DSM correction formulae based on the direct strength method of a laterally braced cold-formed steel channel or zee section purlins. Li, L. Y. (2004) studied analytical models to determine the lateral torsional buckling of Z-purlin laterally restrained by sheeting subject to different cases of loading (pure bending, uniformly distributed gravity and uplift loading) with different boundary conditions using sag rods. He observed that a very efficient method of enhancing the member's resistance to lateral-torsional buckling is to use sag rods. In addition, the energy method is utilized to determine the effect of lateral bracing provided by sheeting on the lateral torsional buckling of a Z-purlin beam with different parameters (boundary conditions, location of load, tie rods) by Chu, X. T., et.al. (2005). It has been found that the loading position most sensitive to the lateral restraint is at the top flange near the web central line. The influence of the lateral restraint on the critical load can be significantly reduced by the presence of anti-sag bars. Moreover, the increase in critical load caused by the lateral restraint is moderate for simply supported beams but quite significant for pinned-fixed beams. Gao, T., and Moen, C. D. (2012), determined the flexural response of simple purlins subject to outward wind loading using the direct strength method. The study demonstrates DSM's accuracy compared to Eurocode and AISI methods, highlighting its conservative predictions, and suggests modifications for improved reliability in Z-section designs. Almatrafi, M., et al. (2021) studied experimentally and numerically the structural behavior of a two Z-sections with lips placed in the opposite direction subjected to four points of downward loading linked to cladding sheeting by fasteners in the presence of angle struts. Moreover, the influence of the length of the lip in the Z section on the flexural strength was considered.

The motivation behind this study is to investigate the variation in the flexural resistance of simply supported parallel purlins laterally braced by tie rods under a gravity loads. The typical detail of roof purlins laterally supported by tie rods is shown in Fig. 1. In this detail, tie rods are connected laterally between purlins in approximately straight lines. They are arranged in zigzag way along this straight line, however, at the last panel, the tie rods are inclined to end them at points directly lay above the frame rafter. Therefor this point is relatively prevented from lateral translation. Spacing between rods depends mainly on the overall span of the purlins.

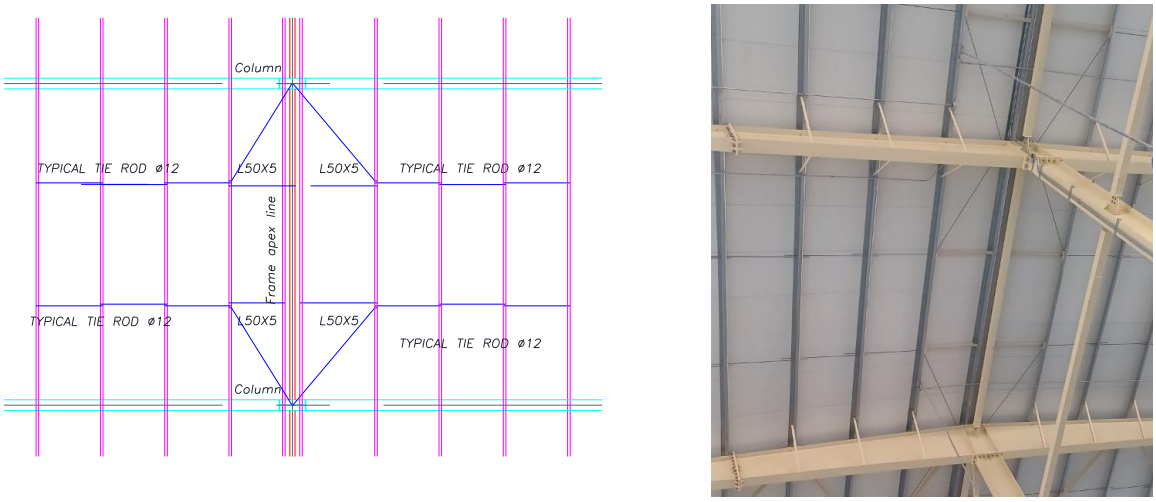

a) Typical detail of tie rods b) Site Photo (El Araby Glass Factory)

Fig.1: Typical detail of purlins with lateral tie rods.

2. Case of Study

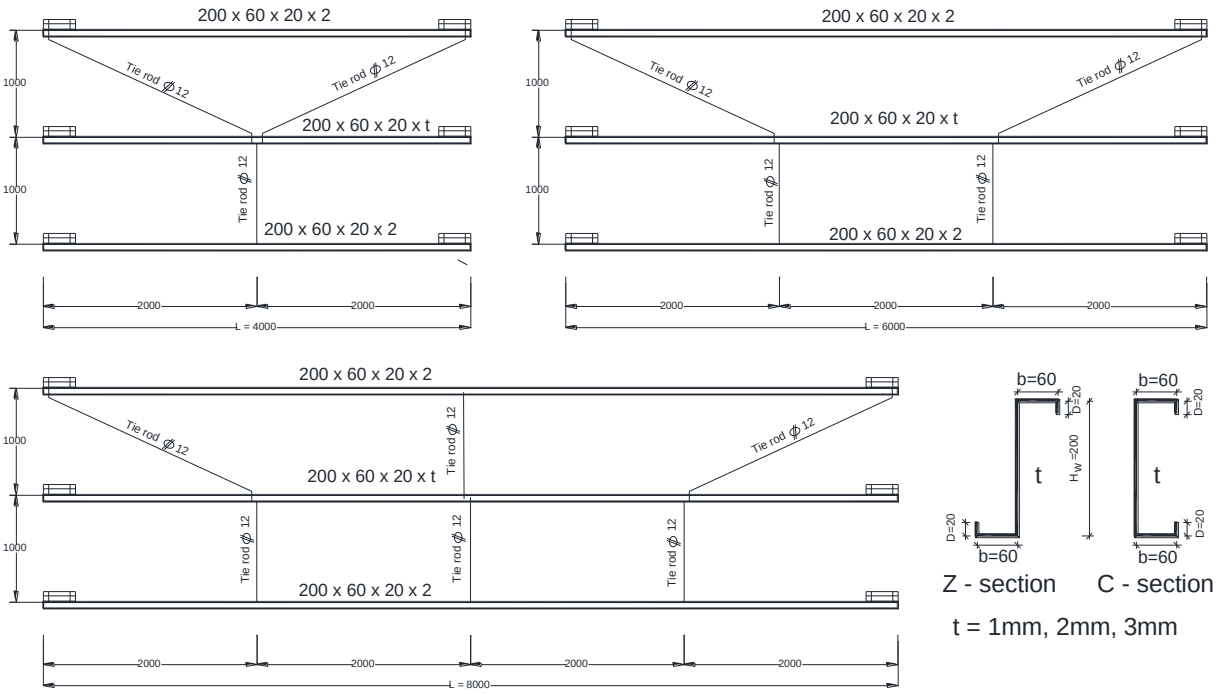

Fig.2 : case of study

The detail shown in Fig.1 has been simulated in this investigation by considering three parallel purlins laterally connected by tie rods as shown in Fig.2. Spacing between purlins is assumed equal 1m. The straight tie rods are connected at the mid height of the web, while the inclined rods are connected at the quarter height of the web from the top flange that is subjected to compression. Three spans are considered which are 4m, 6m, and 8m. For each span the spacing between tie rods

is kept constant equal to 2m. The cross section studied are Zed "Z" and lipped channel "C" sections. The web height, H_w, flange width, b, and lip depth, d, of the cross sections are 200mm, 60mm, and 20mm; respectively. The cross section thickness, t, equal 1mm, 2mm, and 3mm. As the purlin is fixed on the frame rafter using two bolts with spacing between them equal 200mm, the structural model of the purlin is as illustrated in Fig. 3

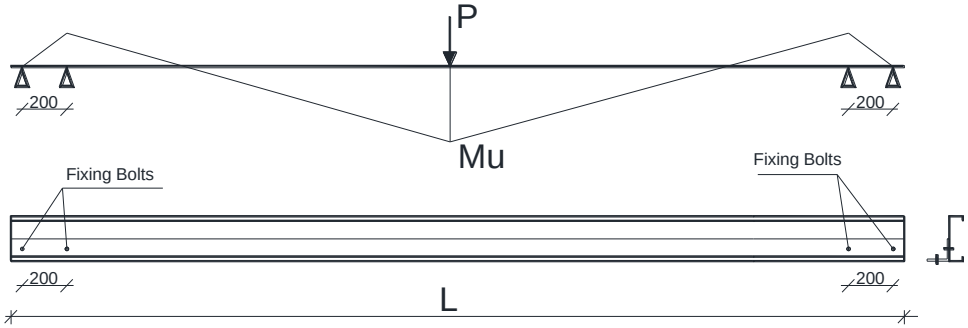

Fig. 3: Structural model of the Studied case

3. Experimental tests and numerical simulation

3.1 Test setup

Six specimens have been tested in this study. Three purlins are tested alone without the tie rods, while the others are connected laterally by the tie rods as shown in Fig. 4. The tested purlins have 4m span, and lipped channel cross section with web depth, H_w, flange width, b, and lip depth equal 200mm, 60mm, 20mm; respectively, while the thickness, t, equal 1mm, 2mm, and 3mm. Table 1 listed the cross section dimensions of the tested specimens.

Table 1: Tested Specimens

Specimens	Measured Diminsions				Pu (KN)		Pu.exp/Pu.fem	Comments
	Hw (mm)	B (mm)	D (mm)	t (mm)	Exp.	F.E.M		
P-1	201	61	19	1.05	4	4.06	0.985	purlins without tie rods
P-2	199	59	19	1.95	11.8	10.6	1.113	purlins without tie rods
P-3	201	59	21	3.2	19.91	20.54	0.969	purlins without tie rods
PT-1	199	61	21	1	6.08	5.92	1.027	purlins with tie rods.
PT-2	199	58	19	1.9	14.89	16.34	0.911	purlins with tie rods.
PT-3	198	58	19	3.1	24.36	24.72	0.985	purlins with tie rods.

The mechanical properties of the CFS used in the specimens were determined according to the ASTM-A370 specifications. Three specimens were tested, and results revel that the steel is high strength steel with yield stresses and Young's modulus equal to 360MPa, and 210 GPa; respectively.

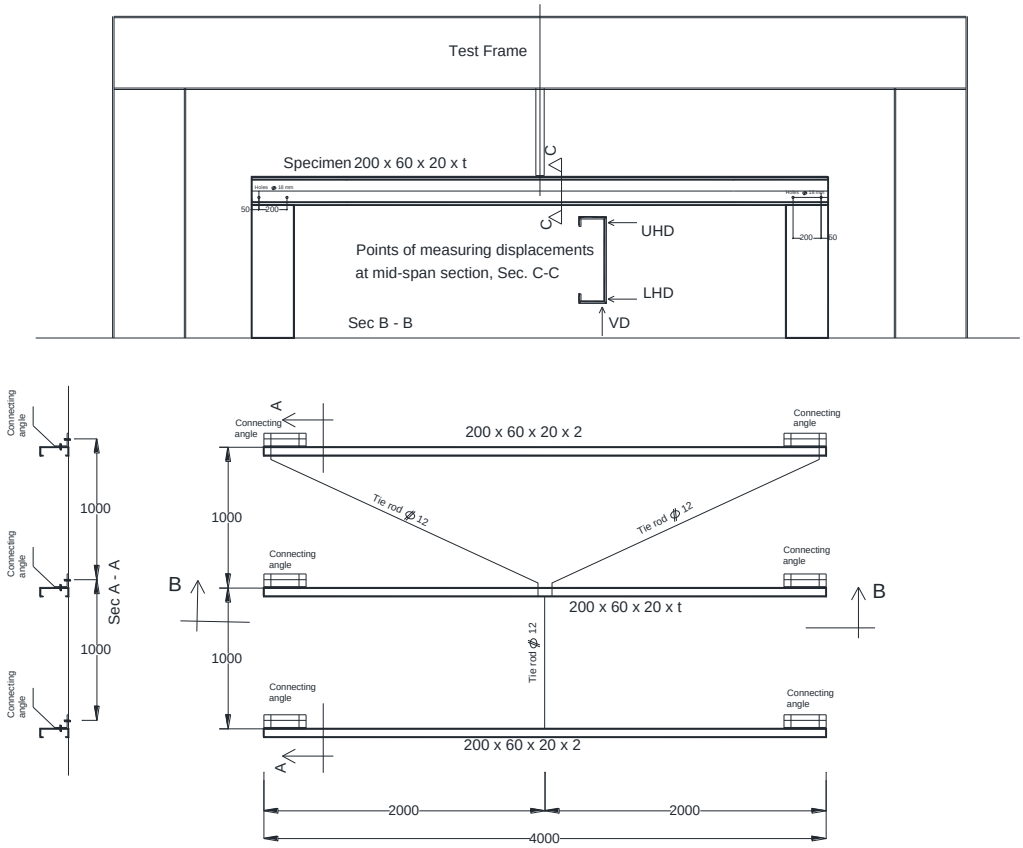

Fig. 4 specimens tested

The specimens are placed horizontally, and supported on two rigid beams using seat angle 100x100x10mm. The distance between the rigid beams is 4m. The concentrated load is applied vertically by 100KN hydraulic jac. The vertical as well as the horizontal displacements of the points at the mid span section where the load is applied are measured using three linear variable displacement transducers (LVDT) with accuracy of 0.01 mm. The measured points were the vertical displacements of the beam mid-span section below the load application (VD), as well as the horizontal displacements of the flange web junction, (UHD) & (LHD). Fig. 5 illustrate the test setup. The LVDT readings were collected using a data acquisition system. An arbitrary increment of load equal to 5kN was applied, and then the load was held constant until stable readings were recorded. This procedure was repeated for each additional load increment until excessive deflections were observed without any increase in the applied load. Thus, the ultimate load was achieved

a) Purlin without tie rod

c) Load application and LVDT's

b) Purlins with tie rods

Fig. 5: Test Setup

3.2 Finite element model

ABAQUS (2012) software is used to develop a nonlinear finite element model for the tested specimens. The linear 4 nodded S4R shell element is used to model the purlins. It is isometric quadrilateral shell element with reduced integration. Further, this element allows for for both geometric and material non-linearties. The element size utilized in the model is fixed at 12mm to achieve sufficiently accurate results, Almatrafi et al., (2021). In addition, the tie rods are modeled by link element with circular cross section area.

A perfect plasticity model based on a simplified bilinear stress-strain curve without strain hardening was assumed in the model. The Young's modulus is considered 210 GPa, and the Poisson's ratio is 0.3. The considered nominal yield strengths are 360 MPa for purlin and 240MPa for tie rods. Young's modulus of elasticity, *E*, and shear modulus, G, are 210 GPa, 81GPa; respectively. The classical metal plasticity model was used to include the material non-linearity effects. This model implements the von-Mises yield surface to define isotropic yielding and

associated plastic flow theory. The boundary conditions at the end sections are such that the horizontal lateral movement (U_x) and the rotation about the longitudinal axis (URz) is prevented along the line of the web only. In addition, the points at which the bolts connect the purlin to the set angle are restraint against translation in the X, Y, and Z directions. The loads are applied in the form of point load at the top flange web juncture. Figure 6 shows the finite element model, loads, and boundary conditions.

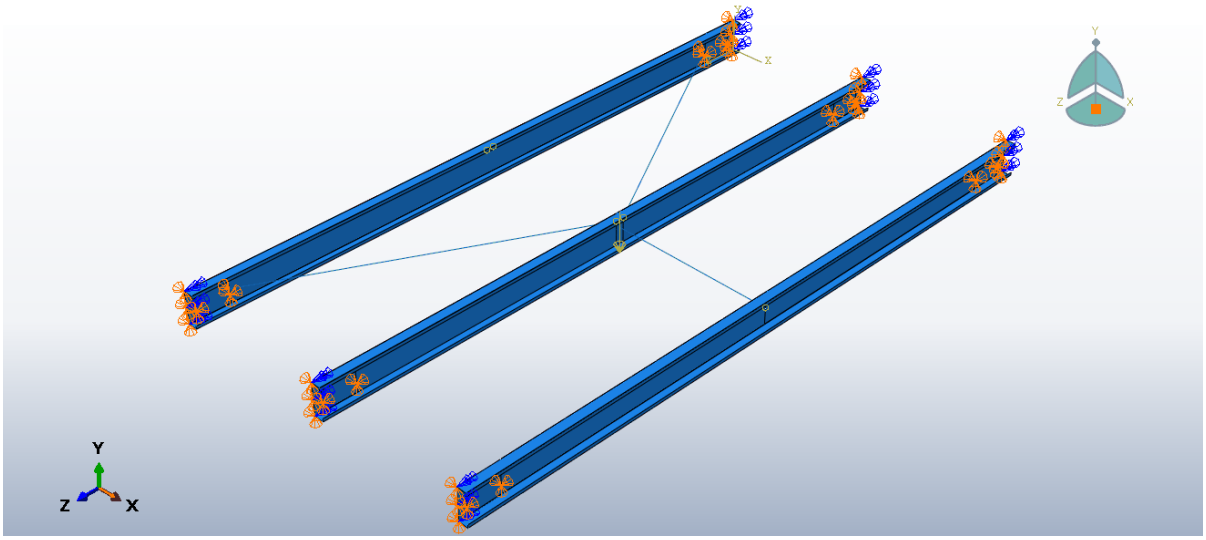

a) Whole Model

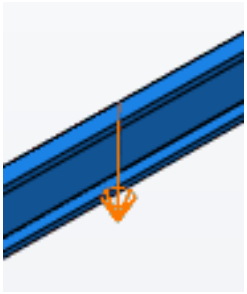

b) Load application

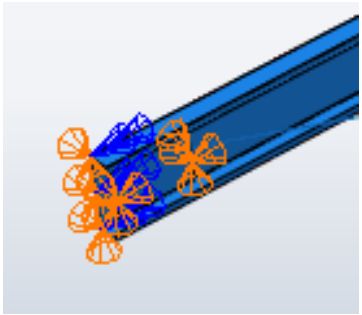

c) boundary conditions

Fig. 6: Finite Element Model

First, linear buckling analysis was done in order to obtain buckling mode shapes. Then the critical buckling shape was scaled by the imperfection value, to be the initial imperfect shape of the non-linear analysis. The considered initial imperfection value is L/1000 for global buckling mode, where L is the length of purlin. However, for local or distortional buckling mode, the value is taken as 0.1t, where t is the thickness of the purlin. Loads were incrementally increased through successive load steps. Newton-Raphson iterations were used in solving the nonlinear system of equations.

3.3 Comparison between experimental and numerical results

In this section, the structural behaviour of purlins laterally supported by tie rods is assed by examining the relation between the vertical applied concentrated loads and the corresponding

horizontal as well as vertical displacements. Results are plotted in Fig. 7, Fig. 8, and Fig. 9 for purlins with thickness t = 1mm, 2mm, 3mm; respectively. Figures also illustrate results of both single purlins, and purlins laterally supported by tie rods. Further, the finite element results are added to the figures. Close observation to the results revel that, for both purlins with or without tie rods, the load vertical displacements relations are almost linear at the early stage of loading. Then near the ultimate loads a sudden drop in the stiffness of the purlins are noticed, and the relations become non-linear till the failure loads. However, a nonlinear relation between the vertical loads and the horizontal displacement are illustrated for the two types of purlins from the early stage of loading. The beams start to deflect in the plane of the web, then near the ultimate loads they start to rotate out of the loading plane. Moreover, the ultimate loads of purlins with tie rods are significantly higher than that without tie rods. The ratio PT_u/P_u = 1.52, 1.26, 1.22 for purlins with 1mm, 2mm, 3mm; respectively. This ratio decreases when the web-width thickness ratio decreases. (Note, PT_u: the ultimate loads of purlins with tie rods, Pu: ultimate loads of purlins without tie rods)

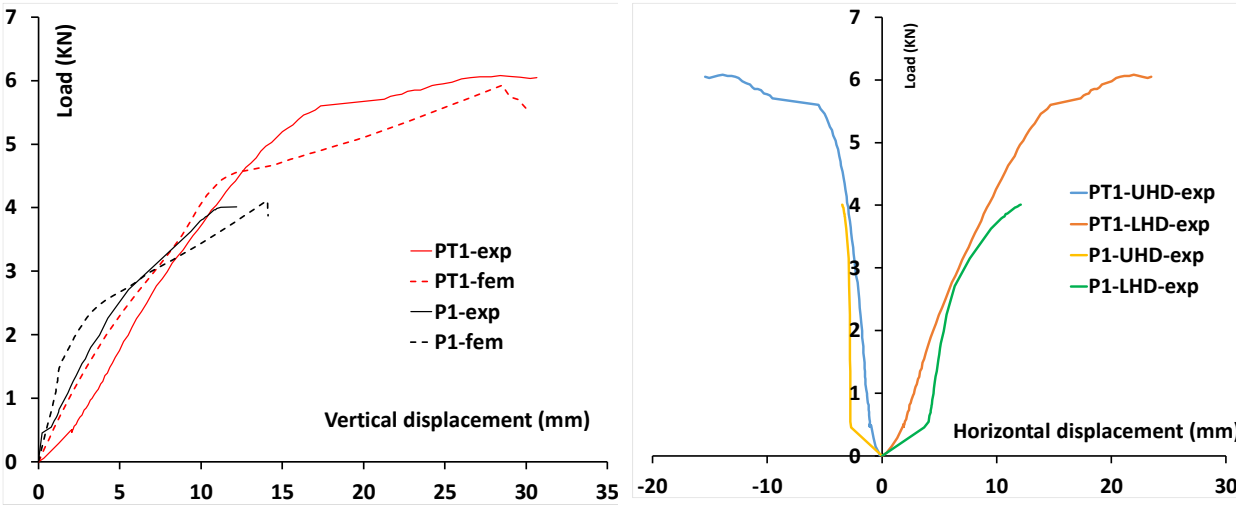

Fig. 7: Vertical Loads, P, versus displacements, of point at mid-span section, C-section, t = 1mm.

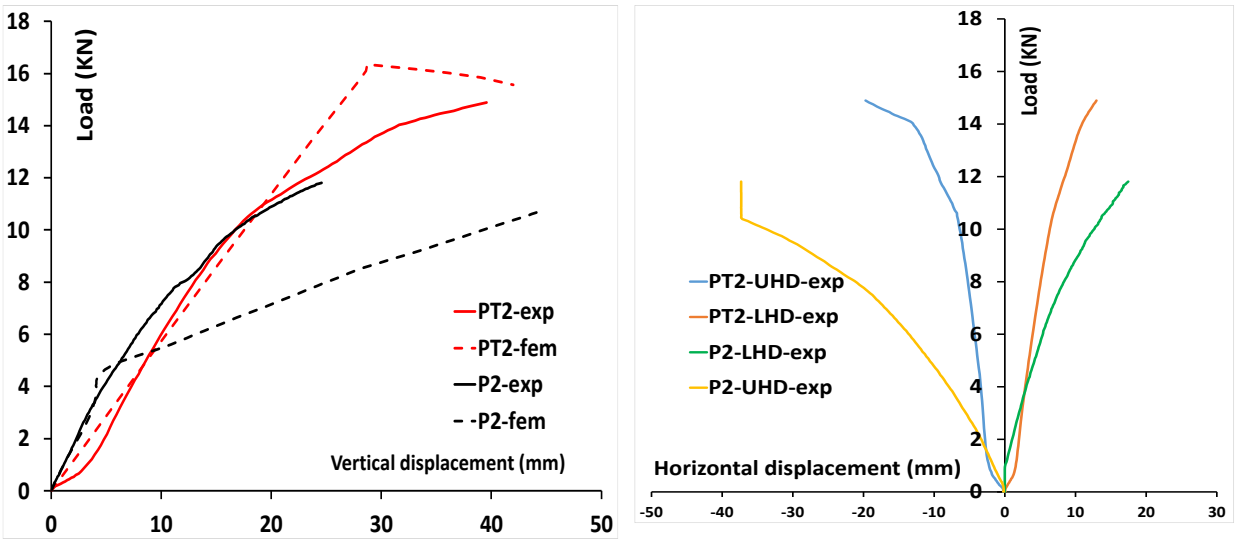

Fig. 8: Vertical Loads, P, versus displacements of point at mid-span section, C-section, t=2mm.

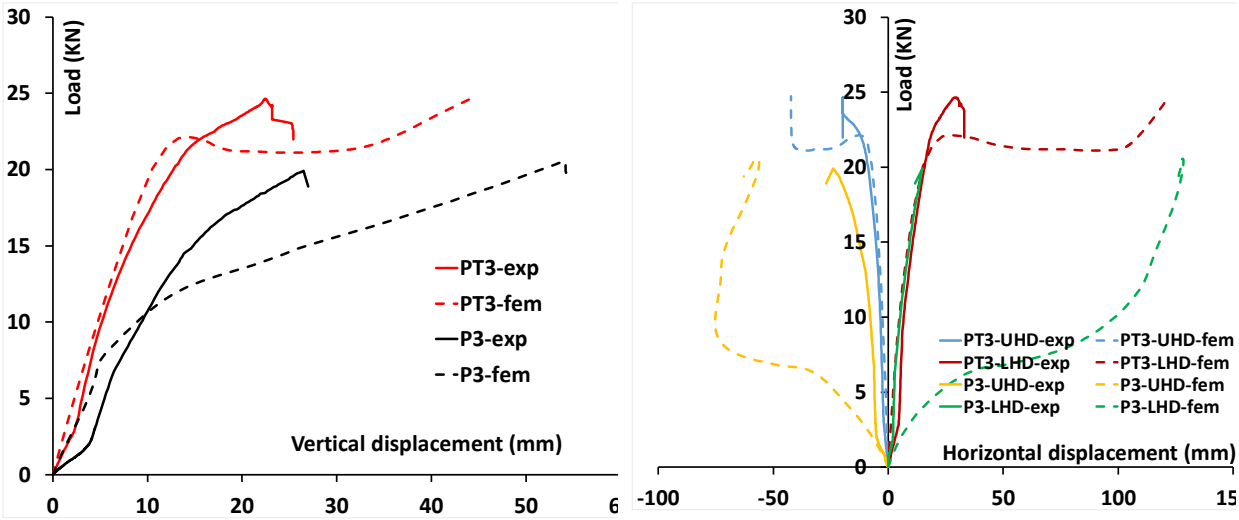

Fig.9: Vertical Loads, P, versus displacements of point at mid-span section, C-section, t=3mm.

Figures also illustrate that the lateral torsionl stiffness of purlins with lateral tie rods are relatively higher than that without tie rods. In addition, the observed failure modes are overall lateral torsional buckling associated with spread of yielding on the top compressive flange as illustrated in Fig. 10 and Fig. 11 for purlins without tie rods, and purlins with tie rods; respectively. Further, the experimental as well as the numerical ultimate loads are comparable. Note, the experimental and finite element results are listed in Table 1 for the tested specimens.

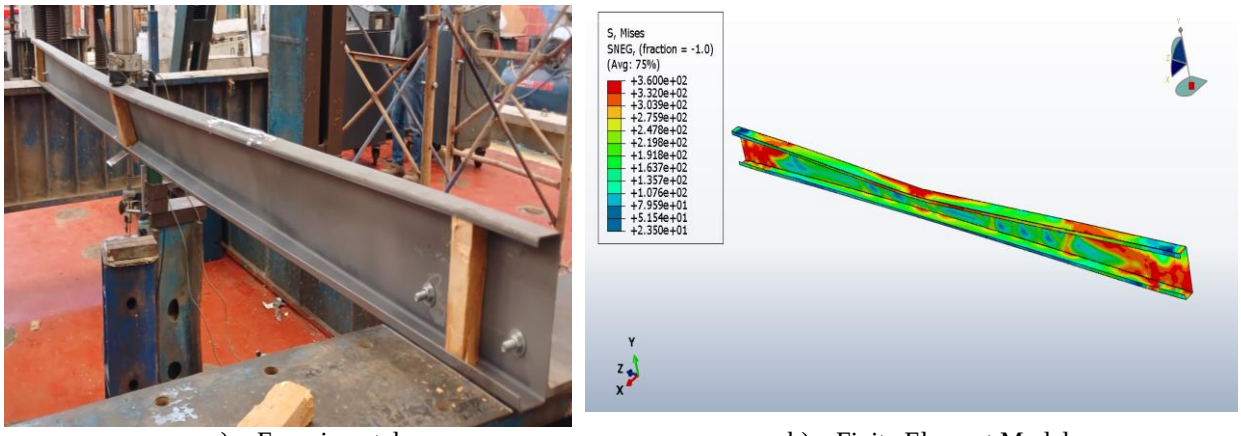

a) Experimental b) Finite Element Model

Fig. 10: Failure modes of purlins without tie rods, specimen P-1, C-section, t=1mm.

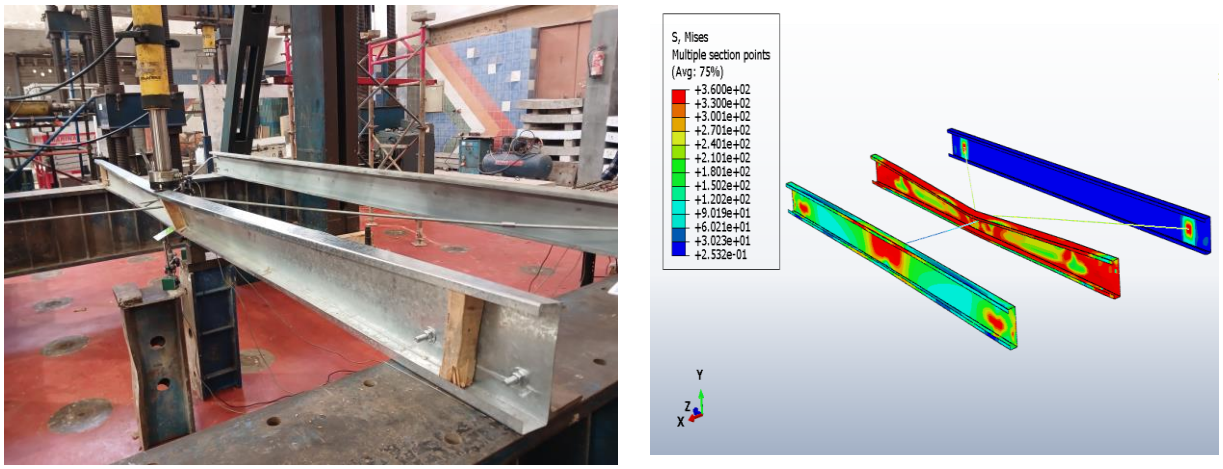

a) Experimental b) Finite Element Model

Fig. 11: Failure modes of purlins with tie rods, specimen PT-1, C-section, t=1mm.

4. Extended parametric study

The developed finite element model is used to determine the ultimate loads of purlins with overall span equal to 6m, and 8m as shown in Fig. 2. The results of C-section purlins and Z-section purlins are listed in Table 2, and Table 3; respectively. It is obvious that using lateral tie rods leads to increase in the ultimate capacity of the purlins. Moreover, this increase in the strength is significant for long span purlins such as 6m and 8m, which reaches 5 times the flexural strength of purlins without tie rods. Further, this additional strength decreases as the web width-thickness ratio decreases. This increase in strength is attributed to the tie rods reduces the lateral unsupported length of the compression flange, and change the failure modes from overall lateral torsional buckling to overall lateral torsional buckling associated with distortional buckling in the compression flanges. This failure mode is clear in purlins with Z-sections. Failure modes of C, and Z section purlins with length 8000mm, and thickness 1mm are depicted in Fig. 12, and Fig. 13; respectively.

Table 2: Ultimate loads, P_u (KN), of C-section purlins

L_b (mm) (1)	t (mm) (2)	$P_{u\ (F.E.M.)}$ (3)	$PT_{u(F.E.M)}$ (4)	$PT_{u(F.E.M)}$ /$P_{u(F.E.M.)}$ (5)	$P_{u(DSM)}$ $L_b = L$ (6)	$P_{u(DSM)}$ L_b = 2000mm (7)
4000	1	4.06	5.9	1.45	4.04	8.34
	2	10.60	16.34	1.50	8.40	24.16
	3	20.54	24.74	1.20	13.50	35.19
6000	1	0.87	4.80	5.50	1.28	5.5
	2	3.20	13.26	4.14	2.70	16.11
	3	4.70	19.56	4.16	4.63	23.46
8000	1	0.57	3.36	5.91	0.56	4.17
	2	2.10	10.60	5.04	1.30	12.08
	3	3.45	12.43	3.60	2.32	17.59

Table 3: Ultimate loads, P_u (KN), of Z-section purlins

L_b (mm) (1)	t (mm) (2)	$P_{u\ (F.E.M.)}$ (3)	$PT_{u(F.E.M)}$ (4)	$PT_{u(F.E.M)}$ /$P_{u(F.E.M.)}$ (5)	$P_{u(DSM)}$ $L_b = L$ (6)	$P_{u(DSM)}$ L_b = 2000mm (7)
4000	1	4.80	6.50	1.35	4.10	8.80
	2	12.30	21.30	1.73	8.20	24.20
	3	18.60	29.20	1.56	12.44	35.12
6000	1	1.20	4.80	4.00	1.26	5.80
	2	3.60	15.70	4.36	2.65	16.10
	3	5.40	20.10	3.70	4.33	23.40
8000	1	0.58	3.20	6.40	0.53	4.40
	2	2.10	11.50	5.50	1.22	12.10
	3	3.30	16.50	5.00	2.12	17.56

The obtained ultimate moments are correlated with that predicted by AISI-2022. In this comparison, the ultimate bending moments, M_u are calculated using the *DSM* approach. In this approach, the flexural strength will be the minimum of the local, distortional, and the overall buckling strength. Note that, calculation of the elastic critical local, distortional, and global buckling stresses have been determined using CUFSM V4.06 computer program. Note, the partial safety factors, γ_{M1}&ϕ_c, are not included when calculating the design loads. The ultimate applied concentrated loads are determined from the corresponding ultimate moments using equation (1)

$$M_u = P_u .L / 8 \quad (1)$$

L = Purlin length

Two values of the ultimate loads, P_u, are calculated by the *DSM*. The first one assuming the lateral unsupported length, L_b, of the purlins compressive flange equal to the total length of the purlin, while the second one assuming L_b = 2000mm (spacing between tie rods). Results are listed in column 6, and column 7. Comparing the *FEM* results with the *DSM* results show that, ultimate loads of purlins without tie rods are slightly higher than that of *DSM* with $L_b = L$. However, for

purlins with tie rods the *FEM* results are near the *DSM* results with L_b equal to the spacing between tie rods. This is due to the tie rods reduces the lateral unsupported length of the compression flange and increase the lateral torsional stiffness of the purlins

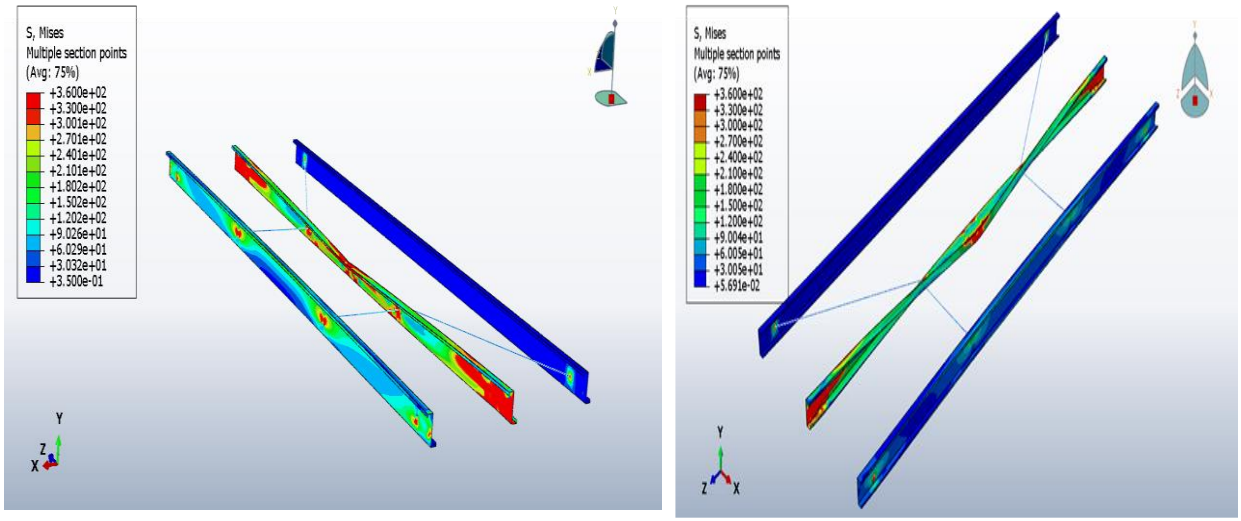

a) Z-section b) C-section

Fig. 12: Failure mode of purlins with tie rods, L = 6000mm, t = 1mm

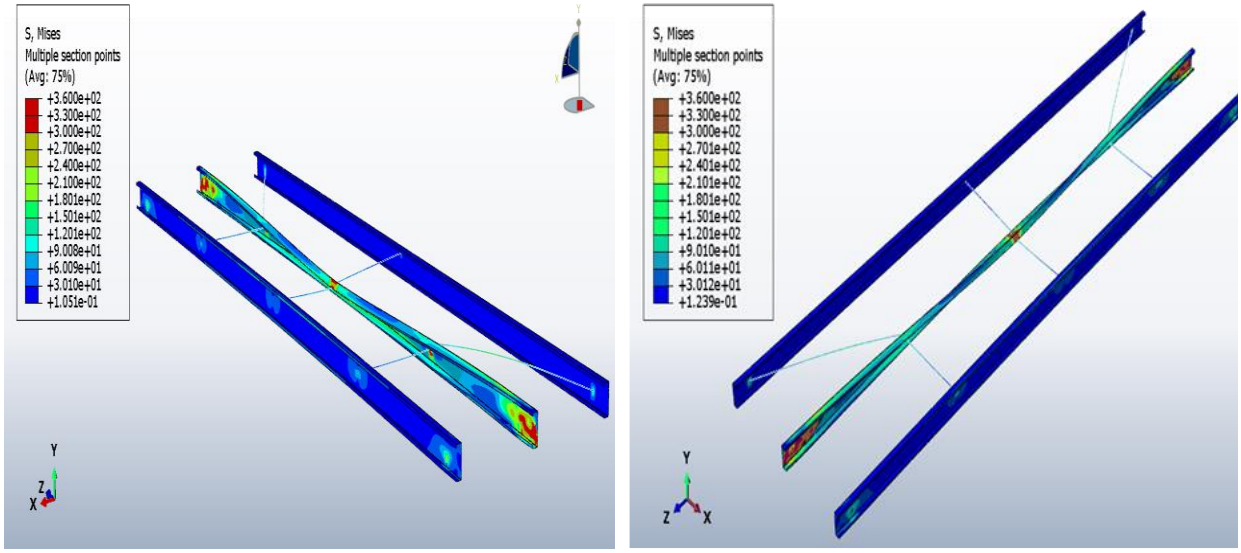

a) Z-section b) C-section

Fig. 13: Failure mode of purlins with tie rods L = 8000mm, t = 1mm

5. Conclusions

The flexural capacities of purlins composed of Zed "Z" or lipped channel "C" cold formed sections, and subjected to concentrated load at the mid-span section have been studied experimentally as well as numerically. Parametric study has been done including section thicknesses as well as the overall member slenderness ratios. Results revel that the presence of tie rods increasing the lateral torsional stiffness of the purlins, in-addition, the failure modes observed are overall lateral torsional buckling associated with distortional buckling waves in the

compressive flanges especially in long span purlins. Further, due to reducing the laterally unsupported length of the compressive flange the flexural strength of purlins with tie rods increases, and could reach 5 times the flexural strength of purlins without tie rods.

Acknowledgments

Authors acknowledge EMCON engineering company for supporting this research through fabricating the tested specimens.

References

Almatrafi, M., Theofanous, M., Dirar, S., & Gkantou, M. (2021). "Structural response of cold-formed lipped Z purlins–Part 1: Experimental investigation." *Thin-Walled Structures*, *161*, 107452.

Almatrafi, M., Theofanous, M., Dirar, S., & Bock, M. (2021). "Structural response of cold-formed lipped Z purlins–Part 2 numerical modelling and optimisation of lip size." *Thin-Walled Structures*, *161*, 107453.

AISI S100-16(R2020) w/S3-22: North American Specification for the Design of Cold-Formed Steel Structural Members, 2016 Edition (Reaffirmed 2020) With Supplement 3, 2022 Edition.

Basaglia, C., D. Camotim, R. Gonçalves, and A. Graça. (2013). "GBT-based assessment of the buckling behaviour of cold-formed steel purlins restrained by sheeting." Thin-Walled Struct. 72: 217–229.

Chu, X. T., Rickard, J., & Li, L. Y. (2005). "Influence of lateral restraint on lateral-torsional buckling of cold-formed steel purlins." *Thin-Walled Structures*, *43*(5), 800-810.

Chu, X.-T., R. Kettle, and L.-Y. Li. (2004). "Lateral-torsion buckling analysis of partial-laterally restrained thin-walled channel-section beams." J. Constr. Steel Res. 60 (8): 1159–1175.

CUFSM v4.06 "Elastic Buckling Analysis of Thin-Walled Members by Finite Strip Analysis, http://www.ce.jhu.edu/bschafer/cufsm.

Dundu, M. (2011). "Design approach of cold-formed steel portal frames." *International Journal of Steel Structures*, *11*, 259-273.

Gao, T., and Moen, C. D. (2012). "Direct Strength Design of Metal Building Wall and Roof Systems-Through-fastened Simple Span Girts and Purlins with Laterally Unbraced Compression Flanges." Proceedings of the 21st International Specialty Conference on Cold-Formed Steel Structures, University of Missouri-Rolla, St Louis, Missouri, USA.

Guimarães, V. M., Gilbert, B. P., Talebian, N., & Wang, B. (2021). Shape optimisation of singly-symmetric cold-formed steel purlins. " *Thin-Walled Structures*, *161*, 107402.

Hibbitt, K. (2012). Inc. ABAQUS. ABAQUS/Standard User's Manual Volumes I-III and ABAQUS CAE Manual.

Li, L. Y. (2004). "Lateral–torsional buckling of cold-formed zed-purlins partial-laterally restrained by metal sheeting." *Thin-walled structures*, *42*(7), 995-1011.

Luan, W., and Li, Y. Q. (2019). "Experimental investigation on wind uplift capacity of single span Z-purlins supporting standing seam roof systems." *Thin-walled structures*, *144*, 106324.

Sokol, L. 1996. "Stability of cold formed purlins braced by steel sheeting." Thin-Walled Struct. 25 (4): 247–268.

Sun, K., G.Tong, and L. Zhang. 2016. "Twisting about constrained line of parallel purlins inter braced by sagrods under wind suctions." Thin-Walled Struct. 108: 30–40.

Tong, G., and Y. Tang. 2017. "Buckling of parallel purlins inter-braced by sag-rods." J. Constr. Steel Res. 139: 123–134.

Ye, J., Hajirasouliha, I., Becque, J., & Pilakoutas, K. (2016). "Development of more efficient cold-formed steel channel sections in bending." *Thin-walled structures*, *101*, 1-13.

Ye, Z.-M., R. J. Kettle, L.-Y. Li, and B.W. Schafer. 2002. "Buckling behavior of cold-formed zed-purlins partially restrained by steel sheeting." Thin-Walled Struct. 40 (10): 853–864.

Zhang, L., and Tong, G. S. (2016). Lateral buckling of simply supported C-and Z-section purlins with top flange horizontally restrained. *Thin-Walled Structures*, *99*, 155-167.

Zhang, Y., Xue, J., Song, X., & Zhang, Q. (2018). "Numerical parametric analysis of the ultimate loading-capacity of channel purlins with screw-fastened sheeting." *International Journal of Steel Structures*, *18*, 1801-1817.

Zhu, Y. J., Zhang, Y. C., & Liu, X. L. (1999). "Several factors affecting the static behavior of diaphragm-braced beams." Journal of Tianjin University, 32(2), 163–167.

Zhang, Y. C., & Wang, H. M. (2009). "Experimental study on bending strength of cold-formed steel C-section members." Journal of Building Structures, 30(3), 53–61.